Supporting Information for Unique hot carrier distributions from scattering mediated absorption

Jason Codrington[†], Noor Eldabagh[†], Kimberly Fernando[†], and Jonathan J. Foley IV[*]

Department of Chemistry, William Paterson University, 300 Pompton Road, Wayne, NJ, 07470, USA

E-mail: foleyj10@wpunj.edu

---

[*]To whom correspondence should be addressed
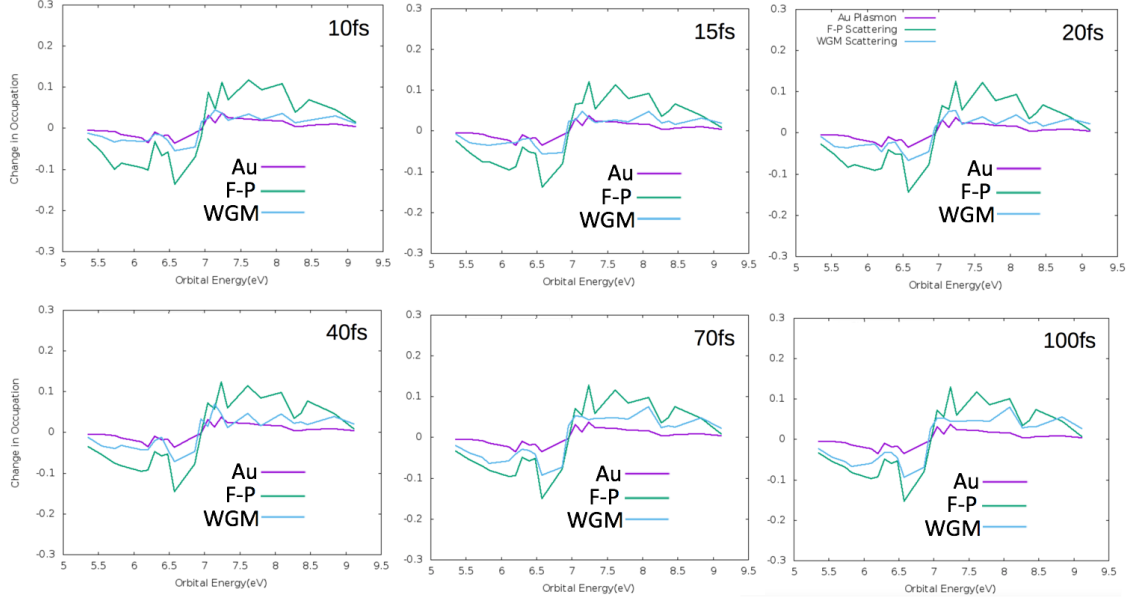
Plots of Global Hot-Carrier Distributions

Figure S1: Snapshots of changes in occupation of each orbital in the active space of the PIW Au NC model as a measure of instantaneous hot carrier distributions. The change in orbital occupation is computed from elements of the time-dependent one-electron reduced density matrix (^{1}RDM) relative to their initial value, $D_p^p(t) - D_P^p(t = 0)$ for several timepoints in the simulation.

Electronic structure of metal nanocubes

For cubic metal nanoparticles, we approximate the one-electron orbitals as energy eigenstates of the particle-in-a-cubic-well. For a particle confined by a cubic well with length L, the potential is 0 when $x < L, y < L, z < L$ and infinity otherwise. The energy eigenstates have the form

$$\psi_{nx,ny,nz} = \left(\frac{2}{L}\right)^{3/2} \sin\left(\frac{n_x \, \pi \, x}{L}\right) \sin\left(\frac{n_y \, \pi \, y}{L}\right) \sin\left(\frac{n_z \, \pi \, z}{L}\right). \tag{1}$$

The energy eigenvalues have the form

$$\epsilon_{nx,ny,nz} = \frac{\hbar^2 \pi^2}{2 \, m \, L^2} \left(n_x^2 + n_y^2 + n_z^2\right). \tag{2}$$
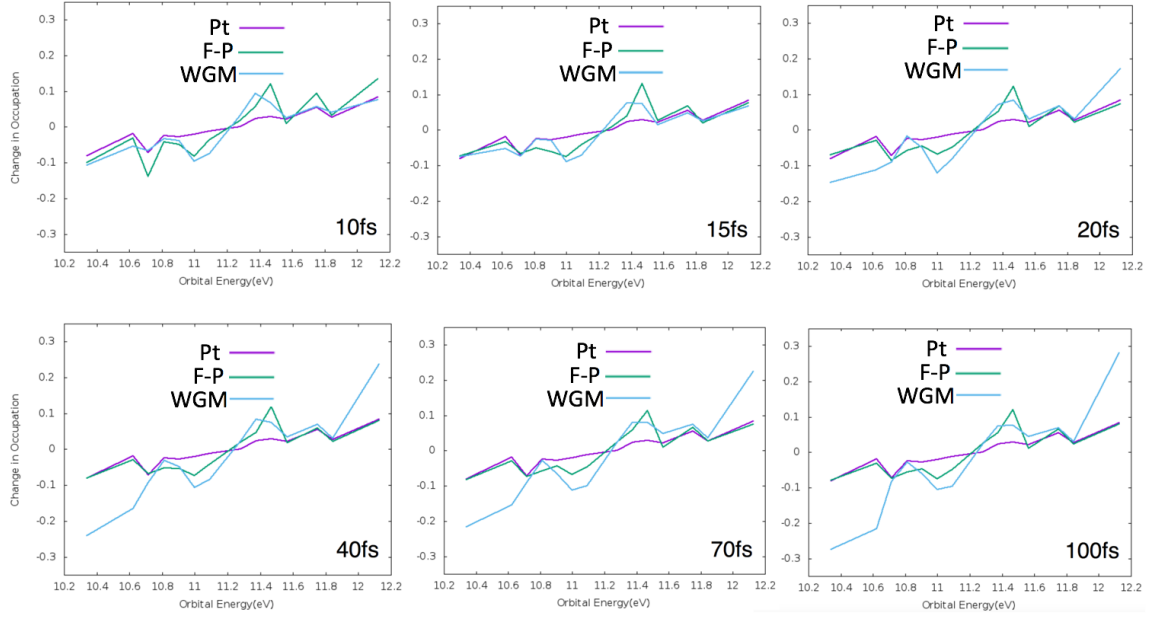
Figure S2: Snapshots of changes in occupation of each orbital in the active space of the PIW Pt NC model as a measure of instantaneous hot carrier distributions. The change in orbital occupation is computed from elements of the time-dependent one-electron reduced density matrix (^{1}RDM) relative to their initial value, $D_p^p(t) - D_P^p(t = 0)$ for several timepoints in the simulation.

The transition dipole operator can be decomposed into its components,

$$\hat{\mu} = \hat{\mu}_x \, \mathbf{i} + \hat{\mu}_y \, \mathbf{j} + \hat{\mu}_z \, \mathbf{k}. \tag{3}$$

The transition dipole integral components can be evaluated analytically, for example, the x-component has the form

$$\langle \psi_{nx,ny,nz} | \hat{\mu}_x | \psi_{nx',ny',nz'} \rangle = e \, \delta_{ny,ny'} \, \delta_{nz,nz'} \, \frac{L(\pi(n_x - n_x')\sin(\pi(n_x - n_x')) + \cos(\pi(n_x - n_x')) - 1)}{\pi^2(n_x - n_x')^2}$$

$$- e \, \delta_{ny,ny'} \, \delta_{nz,nz'} \, \frac{L(\pi(n_x + n_x')\sin(\pi(n_x + n_x')) + \cos(\pi(n_x + n_x')) - 1)}{\pi^2(n_x + n_x')^2},$$

where $\hat{\mu}_x = -ex$. Analogous expressions can be obtained for expectation values of $\hat{\mu}_y$ and $\hat{\mu}_z$.

We order the orbitals by a single index p such that $\epsilon_{p+1} \geq \epsilon_p$; that is, each $\psi_{nx,ny,nz}$ can be uniquely labeled ψ_p. Using the above expressions and following this labeling scheme, the diagonal matrix elements can be evaluated as

$$\langle \Phi_0 | \hat{H}(t) | \Phi_0 \rangle = \sum_{p=1}^{nocc} \epsilon_p \tag{4}$$

$$\langle \Phi_i^a | \hat{H}(t) | \Phi_i^a \rangle = \sum_{p=1}^{nocc} \epsilon_p - \epsilon_i + \epsilon_a \tag{5}$$

and the off-diagonal matrix elements can be evaluated as

$$\langle \Phi_0 | \hat{H}(t) | \Phi_i^a \rangle = \mathbf{E}(t) \cdot \langle \psi_i | \hat{\mu} | \psi_a \rangle \tag{6}$$

$$\langle \Phi_i^a | \hat{H}(t) | \Phi_j^b \rangle = \mathbf{E}(t) \cdot \langle \psi_a | \hat{\mu} | \psi_b \rangle \delta_{ij} - \mathbf{E}(t) \cdot \langle \psi_i | \hat{\mu} | \psi_j \rangle \delta_{ab}. \tag{7}$$

Finite-difference time-domain calculations

A commercial simulator based on the finite-difference time-domain method[1] was used to compute the electric field, $E(t)$ 1 Å away from the nanoparticle surface in each of the scenarios considered. The displacement was taken along the z-axis, corresponding to the polarization direction of incident light since the strongest near-field enhancement is expected along this direction. A grid spacing of 1 Å in x, y, and z was utilized in a cubic region extending 1 nm beyond the metal NP surface, and a non-uniform mesh was utilized otherwise with dx, dy, $dz \leq 20nm$. For each composite structure, a nanoparticle was placed at the surface of the dielectric nanosphere at an angle of $20°$ with respect to the propagation axis of the incident light. In all simulations, light propagates along the x axis and is polarized along the z axis. The metal nanoparticles are centered at $y = 0$. A total-field scattered-field source was used to illuminate the structures. The FDTD simulations were terminated when the ratio of the total energy in the simulation volume to the total energy injected by the illumination source falls below 10^{-6}. Because the WGMs are higher quality factor resonances, longer time is typically required for these simulations as compared to the plasmonic particles alone.

The resulting time-domain fields were fed into our TDCIS algorithm, allowing us to simulate the electronic dynamics driven by rigorously-computed nearfields from scattering and plasmon resonances, which show strong spatiotemporal modification relative to freely propagating light. The electric field was scaled by a factor $E_0 \approx 614,000,000 \ V/m$ so that the peak power of the illumination source is $10^{15} \ W/m^2$. The electric field was sampled at intervals of approximately 2.8 attoseconds for all simulations, which leads to a time-step that ensures stability of the wavefunction propagation with the relevant energy scales of our simulations. Our TDCIS scheme requires the evaluation of the electric field at intermediate times between these timesteps, and we use a simple update based on centered-finite differences to approximate the electric fields at these times. As an example, if the electric field is known at times t_1, $t_2 = t_1 + dt$, and $t_3 = t_1 + 2 \cdot dt$ where $dt = 2.8 \ as$, and knowledge of the field is required at some time $t_m = t_2 + m \cdot dt$ where m is non-integer, $E(t_m)$ is estimated as

follows:

$$\mathbf{E}(t_m) = \mathbf{E}(t_2) + \frac{\mathbf{E}(t_3) - \mathbf{E}(t_1)}{t_3 - t_1} \cdot m \cdot dt. \tag{8}$$

The optical response of Au and Pt in the FDTD simulations utilizes permittivity data from the work of Johnson and Christy[2] and Palik,[3] respectively. We assume a static dielectric constant of 2.6 for the dielectric nanospheres in this work, which is comparable to the visible dielectric constant of titanium dioxide.

References

(1) Lumerical Solutions, Inc., `http://www.lumerical.com/tcad-products/mode/`.

(2) Johnson, P. B.; Christy, R. W. Optical constants of noble metals. *Phys. Rev. B* **1972**, *6*, 4370.

(3) Palik, E. D. *Handbook of optical constants of solids*; Academic Press, 1998.